

# Reflection High-Energy Electron Diffraction

Nassim Derriche, Simon Godin, Rysa Greenwood, Alejandro Mercado, Ashley Nicole Warner  
*University of British Columbia*

(Dated: November 22, 2019)

In this paper, we present an overview of the diffraction technique known as reflection high-energy electron diffraction (RHEED). We discuss an elementary approach behind the analysis of experimentally obtained RHEED patterns (including patterns we produced at the Stewart-Blusson Quantum Matter Institute). Meaningful information, such as atomic structure and surface topology, can be extracted from this technique. Furthermore, an explanation of the kinematic scattering theory is reviewed and an introduction to the effect of dynamic scattering through the observation of Kikuchi lines is given.

## INTRODUCTION

Reflection high-energy electron diffraction (RHEED) is a relatively inexpensive characterization technique with geometry that is compatible with complicated experimental apparatus. First implemented in the late 1920s, RHEED uses an electron gun to project electrons at a sample and measures the diffraction of those electrons on a fluorescence screen. Electrons penetrate only a few Å into a sample unlike X-ray diffraction (XRD) which measures the bulk of the material. High energy electrons are more easily focused via electromagnetic fields further making RHEED a prime candidate for thin films and various other surface studies [1]. After almost 100 years of use, RHEED has become an effective tool in monitoring the state of materials *in situ* with pulsed laser deposition, molecular beam epitaxy (MBE), atom deposition, scanning tunneling microscopy and various other ultrahigh vacuum apparatus [1, 2].

The three main components of a RHEED experiment are an electron gun, a sample with a pristine surface, and a fluorescence screen, as shown in Figure 1. The electron beam is set to an energy value that can range from 8keV to 100keV, and hits a sample at a fairly low incident angle, usually ranging between  $1 - 4^\circ$ . A low incident angle is crucial in studying surface disorder of the system [1]. A typical RHEED set up will use magnetic fields to change the incident angle of the incoming electrons as well as adjust the diffraction angle by rotating the sample along its azimuth [2].

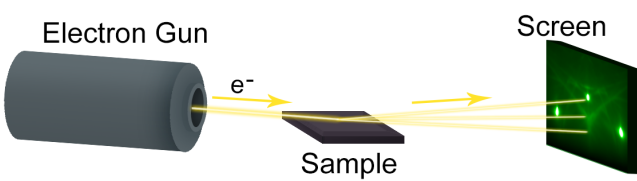


FIG. 1. The simplest RHEED set up includes an electron gun, a sample, and a fluorescence screen across from the gun.

Other diffraction techniques such as low energy electron diffraction (LEED) and XRD, perform similar measurements, but all have distinct strengths and weaknesses in various areas. LEED uses electrons at approximately 10-100eV and the detector is nearly at normal incidence to the sample to collect back scattered electrons [2]. On the other hand XRD photon energies can range from 100eV to 100keV while tending to be more precise and have higher angular resolution than both RHEED and LEED [3]. With the absence of Coulomb interactions in XRD the photons penetrate deeper into the material and provide details of the bulk rather than just the surface [4]. LEED and RHEED are both ultrahigh vacuum compatible, whereas XRD measurements will need to happen *ex situ* as the only source of X-rays powerful enough to compare with RHEED results are at synchrotron facilities. Electrons interact more strongly with matter than X-rays which attributes to RHEED having a higher surface sensitivity and allows time efficient observations of changes in surface level disorder [3]. In addition, if the sample needs to be heated, LEED measurements must wait until the sample is cool as the screen will become over-saturated with thermal energy. The geometry in a RHEED apparatus avoids this problem as the screen can be placed 20cm away, thus collecting no thermal noise [2]. This makes RHEED a useful tool to monitor crystal and thin film growth. Table 1 highlights key differences among the three experimental techniques.

TABLE I. Comparison of RHEED, LEED and High-Energy XRD techniques.

	RHEED	LEED	HE XRD
Source	Electron Gun	Electron Gun	Synchrotron
Energy	8-100keV	10-100eV	10-100keV
Depth	Surface	Surface	Bulk
Site	<i>in situ</i>	<i>in situ</i>	<i>ex situ</i>
Incident $\theta$	$1 - 4^\circ$	$\lesssim 90^\circ$	$1 - 4^\circ$

## DIFFRACTION AND EWALD CONSTRUCTION

It is helpful to describe diffraction experiments such as RHEED with the use of a Fourier transform approach [5]. Some approximations can be made to easily understand the basics of RHEED. The following are assumed in this section:

- Electron collisions are elastic.
- Electrons do not penetrate deep into the material (a few unit cells).
- The material's width is large compared to the coherence length of the electron beam.

These three approximations give rise to the main features in the RHEED pattern. Some of these approximations will be dropped in the following sections which will give rise to much richer physics.

The conditions to observe constructive interference of the outgoing electrons in a RHEED experiment are best determined and visualized by the von Laue formulation and the Ewald construction. Consider diffracted electrons from a lattice plane with incoming momentum  $\mathbf{k}_0$  and outgoing momentum  $\mathbf{k}_i$ . The Laue condition and conservation of energy read [6]:

$$\mathbf{K}_i = \mathbf{k}_i - \mathbf{k}_0, \quad (1)$$

$$|\mathbf{k}_i| = |\mathbf{k}_0|. \quad (2)$$

These conditions are pictured in reciprocal space by the Ewald construction. When using RHEED, the  $\mathbf{k}$ -vectors length is set by the electron gun energy and can be considered to all have the same magnitude. The Ewald sphere is the sphere with radius  $|\mathbf{k}_0|$ . The intersection of this sphere with the reciprocal lattice reproduces the pattern that will be seen on the fluorescence screen. A simple example is the case of a perfectly flat sample with

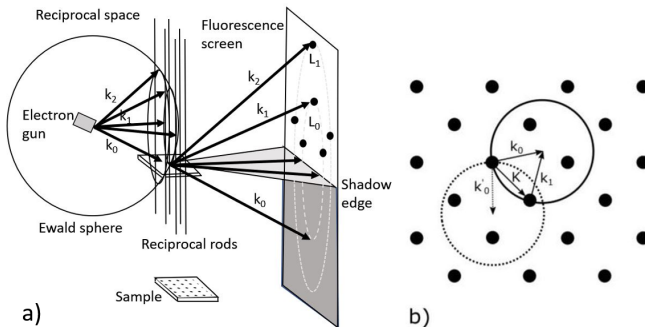


FIG. 2. a) Ewald construction for a 2D plane in reciprocal space and as seen on the RHEED fluorescence screen [2]. b) 2D representation of the Ewald sphere. The solid line circle shows constructive interference for a particular sample angle.

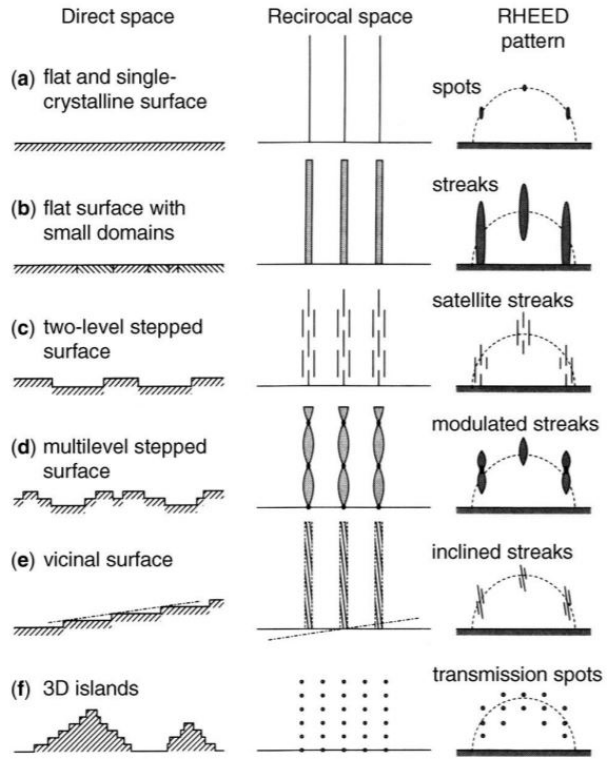


FIG. 3. Different RHEED patterns, where only the lowest Laue zone is shown. Each row shows the effect of different surface defects on the reciprocal space patterns [2].

an infinite 2D square lattice. If we look at the 2D lattice in reciprocal space, we get infinite rods perpendicular to the sample. These rods intersect with the Ewald sphere, reproducing a pattern of concentric dots as shown in Figure 2 [2]. The intensity  $I$  of the pattern is found from the conservation equations (1 and 2) as a sum over all scatterers at positions  $R_{nm} = na\hat{x} + ma\hat{y}$ . This is given by:

$$A(\mathbf{K}) = \sum_{nm} f e^{i\mathbf{K} \cdot \mathbf{R}_{nm}}, \quad (3)$$

$$I = AA^*, \quad (4)$$

where  $A$  is the diffracted amplitude and  $f$  is the scattering factor that depends on the sample's nature. The effect of the rotational degree of freedom in the sample on the RHEED pattern provides information about the structure of the sample. The rotation of the sample can be seen as a rotation of the Ewald sphere, as seen in Figure 2b. Another way to capture the different interference patterns is to change the amplitude vector  $\mathbf{k}_0$ . However, this is not used since it is experimentally challenging to generate electrons over a continuous range of energy.

Let's now discuss the surface information that can be extracted from RHEED patterns. As seen in Figure 3,

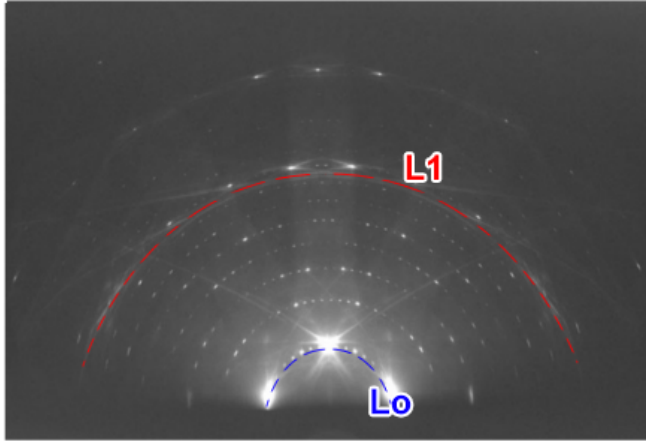


FIG. 4. Near ideal RHEED pattern of Si(111)7×7 measured at a glancing angle of 2.7° [1]. The zeroth (blue) and first Laue zones are the bright circles highlighted in the image, with 6 diffraction circles between them originating from the 7×7 reconstruction.

the RHEED pattern is drastically different for distinct surfaces which shows the surface sensitivity of RHEED [7]. We can consider the case of a two-level stepped surface in Figure 3c. The material will create the rods in reciprocal space as it occurs in the case for a flat material. However, since the electrons only interact with the surface of the material (at least to a good enough approximation), the electrons that hit the lower terraces experience a longer path than the electrons that hit the upper terraces. This difference in path length is described by the Bragg diffraction condition:

$$2d \sin(\theta) = n\lambda, \quad (5)$$

where  $d$  is the height difference between the terraces,  $\theta$  is the glancing angle and  $\lambda$  is the wavelength of the electrons. These differences in the path of the electrons will split the rod into two sharp rods in the off-Bragg condition and will be unaffected in the on-Bragg condition [2].

### REAL RHEED PATTERNS

Experimentally measured RHEED patterns can exhibit a wide range of features associated with surface imperfections. This section will cover real RHEED patterns from the near ideal case of the Si(111)7×7 reconstruction and some common surface defects. Surface reconstruction is the process where topological atoms assume a different structure than the bulk in order to minimize surface energy. The reconstructed surface unit cell is described as multiples of the non-reconstructed unit cell which has vectors  $\mathbf{a}_1$  and  $\mathbf{a}_2$ . So, the  $(m \times n)$  reconstructed unit cell has unit vectors  $m\mathbf{a}_1$  and  $n\mathbf{a}_2$ .

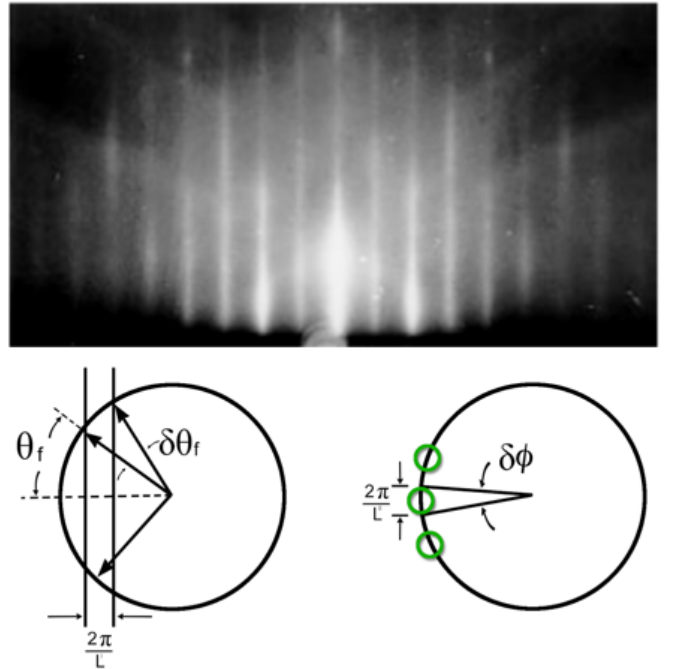


FIG. 5. Top: RHEED pattern from GaAs(001)2×4 reconstructed surface [1]. Bottom: Left) Ewald reconstruction depicting the range of angles  $\delta\theta_f$  in the diffracted beam.  $L'$  is the domain diameter along the direction of the incident beam. Right) Width of the RHEED streaks due to the domain size perpendicular to the direction of the incident beam [5].

For electron diffraction techniques, a surface can be considered atomically flat and a single crystal even when there are different terraces assuming the widths of the terraces are smaller than the coherence length of the electron beam [1]. The Si(111)7×7 reconstruction contains perfect terraces whose widths are typically larger than 300nm and, in some cases, as large as 1000nm [1]. The distance that electrons interfere coherently for the typical electron gun used in RHEED is approximately 1000nm [1]. Therefore, the RHEED pattern from Si(111)7×7 is approximately the ideal case. Figure 4 depicts a real RHEED pattern from the Si(111)7×7 reconstruction. As expected from the discussion of the ideal case in the previous section, the diffraction spots appear in semicircles which correspond to different Laue zones. The radius of the zeroth Laue zone must be  $l \tan(\theta_i)$ , where  $l$  is the distance from the sample to the screen and  $\theta_i$  is the glancing angle of incidence [2].

A common defect seen in RHEED patterns is for the diffraction spots to appear as streaks, as depicted in the top of Figure 5. This is usually caused when the uppermost atomic layers of the surface have limited long range order [1]. An illustration of this is given by Figure 3b, which depicts an atomically flat surface containing multiple domains whose widths are smaller than the coherence length of the electron beam. In this case, the reciprocal rods broaden and their intersection with the

Ewald sphere forms the diffraction streaks [5]. A corresponding Ewald construction is illustrated in the bottom of Figure 5. The resulting (00) streak, which is the streak with the greatest intensity, will have length

$$\delta\theta_f = \frac{2\pi}{L' k \sin\theta_f},$$

where  $\theta_f$  is the grazing departure angle and  $L'$  is the domain diameter along the direction of the incident beam [5]. The angular width will be given by

$$\delta\phi_f = \frac{2\pi}{L'' k \cos\theta_f},$$

where  $L''$  is the domain size perpendicular to the incident beam [5]. Thus, by measuring the length and width of the (00) streak, it is possible to estimate the average size of the domains in the surface.

An extreme case to be considered is a film forming islands on a substrate that are rough enough to become 3 dimensional, as depicted in Figure 3f. In this case, since the glancing angle of the electron beam is small, the electron beam transmits through the island. This results in the diffraction pattern no longer being a reflected pattern but a transmission pattern. The diffraction pattern will then be one that is normal for 3D structures: an array of transmission spots. Figure 6 shows an example of this from data taken from the Ke Zou MBE lab at UBC. Bismuth is deposited on sapphire, which are both expected to have hexagonal structure. The sapphire substrate shows a nearly ideal RHEED pattern. After bismuth deposition however, weak transmission spots are observed and the sapphire spots are still visible. This means that unconnected 3D bismuth islands were grown, with some of the substrate still bare. Further information about the lattice parameter of the bismuth film can be extracted assuming we know the lattice parameter of sapphire (4.754 Å). We know that distances in reciprocal space are inversely proportional to those in real space, so we can compare distances between sapphire features ( $d_{sapp} \approx 1400$  pixels) and bismuth features ( $d_{bi} \approx 1345$  pixels) in order to calculate bismuth's lattice constant:

$$a_{bi} = a_{sapp} \left( \frac{d_{sapp}}{d_{bi}} \right)^{-1} \approx 4.754 \text{ Å} \left( \frac{1400}{1345} \right)^{-1} \approx 4.567 \text{ Å}.$$

This is slightly larger than the bulk lattice parameter of bismuth in that direction, which is 4.54 Å.

Thus far we have only considered elastically scattered electrons, but inelastically scattered electrons also play an important role in the make up of a RHEED pattern.

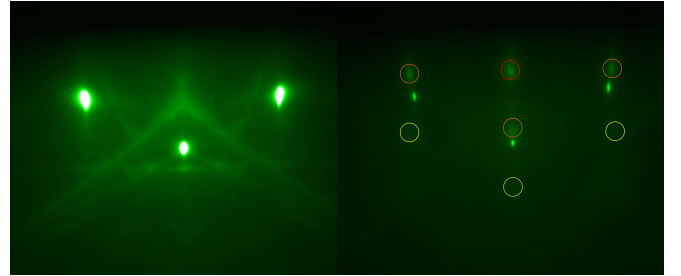


FIG. 6. Left) RHEED pattern of sapphire focused in the center of  $L_0$ . Right) Same RHEED after deposition of 5 unit cells depth of bismuth still show sapphire features and transmission spots for bismuth. The shadow edge is at the top in this figure.

### INELASTIC ARTIFACTS IN RHEED - KIKUCHI LINES

Analysis of artifacts appearing on RHEED images caused by inelastic events yields meaningful data. Such patterns, which are called Kikuchi lines, manifest themselves as lines of varying intensity on RHEED pictures, as can be seen in Figure 6. This section is focused on explaining the origin of these lines qualitatively and how to extract information from them; thorough exploration of the dynamical scattering theory in RHEED is done in specialized literature [8].

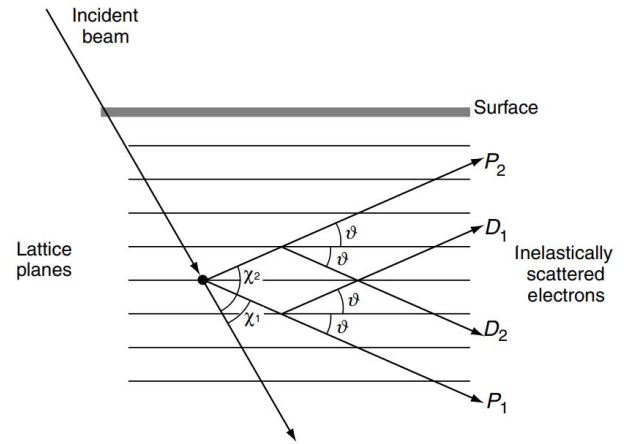


FIG. 7. Diagram of the outgoing electron beams originating from inelastic scattering events producing Kikuchi lines in RHEED images [1].

In the cases when incident electrons penetrate the surface of the sample being studied, they can be inelastically scattered, mainly by thermal diffuse scattering (interaction with lattice vibrations) in any direction. Looking at Figure 7, the orientation of an arbitrary resultant electron beam  $P_1$  respects the Bragg diffraction condition for a specific family of lattice planes in the bulk lattice, producing an elastically scattered electron beam  $D_1$ . The

combination of the fluorescent points produced by all the allowed  $D_1$  points will result in a Kikuchi line associated with the family of planes linked to the diffraction itself, which is why lines can be identified with Miller indices  $(hkl)$ . Geometrically, for the same family of planes, there is always another incident beam direction respecting the Bragg condition (labelled as  $P_2$ ), which leads to another, parallel Kikuchi line with the same  $(hkl)$  caused by the allowed  $D_2$ . Due to more complicated scattering processes, we observe Kikuchi bands with a certain width instead of two parallel lines on RHEED images [9].

The observed Kikuchi pattern depends on the lattice planes which are not parallel to the direction of the electrons shot on the sample. Consequently, Kikuchi lines encode information about the orientation of the lattice, which is controlled experimentally with the azimuthal angle. An azimuthal rotation of the sample causes a continuous transformation of the observed Kikuchi lines, allowing experimentalists to determine lattice orientation in space by fitting theoretical Kikuchi patterns produced by different crystal surface geometries to the ones present on the fluorescence screen.

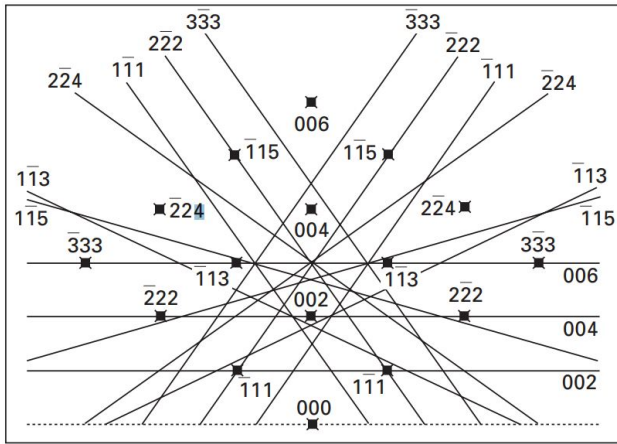


FIG. 8. Diagram of Kikuchi lines for the reciprocal lattice of the (001) surface of an FCC lattice along for a [110] azimuthal RHEED direction [9].

In order to determine all the potential Kikuchi lines for a certain azimuthal angle corresponding to a direct space direction  $[hkl]$ , the reciprocal lattice points with directions  $(h'k'l')$  perpendicular to  $[hkl]$  can be drawn. Since the electrons are ultimately Bragg diffracted, their incoming and outgoing momenta must respect Equations 1 and 2. Consequently, the corresponding Kikuchi lines are then the perpendicular bisectors of the lines connecting the (000) reciprocal lattice point to all the other

points drawn; these lines are projections of great circles on Ewald spheres [9]. The result of this approach is shown in Figure 8: the Kikuchi pattern for the reciprocal lattice points of the (001) surface of an FCC lattice which are perpendicular to the sample direction [100] is constructed. This is the most common and straightforward use of Kikuchi patterns in RHEED experiments.

## CONCLUSION

RHEED is an effective and low-cost imaging technique that is often used *in situ* to monitor sample growth due to its non-intrusive design, mainly used in MBE apparatus. While we presented an overview of this technique, much more can be extracted from RHEED patterns. For example, recreation of the lattice of the sample directly from Kikuchi line analysis is possible [8]. Also, monitoring the evolution of the RHEED pattern during sample growth in real time gives additional insight on the growth behavior. [1]

- 
- [1] Ayahiko Ichimiya and Philip I. Cohen. *Reflection High-Energy Electron Diffraction*. 2004.
  - [2] Shuji Hasegawa. *Characterization of Materials (Second Edition)*, chapter Reflection High-Energy Electron Diffraction, pages 1925–1938. 2012.
  - [3] S. M Suturin, A. M. Korovin, V. V. Fedorov, G.A. Valkovsky, M. Tabuchi, and N. S. Sokolov. An advanced three-dimensional rheed mapping approach to the diffraction study of Co/MnF<sub>2</sub>/CaF<sub>2</sub>/Si(001) epitaxial heterostructures. *Journal of Applied Crystallography*, 46:1532–1543, 2016.
  - [4] P.H. Fuoss and I. K. Robinson. Apparatus for x-ray diffraction in ultrahigh vacuum. *Nuclear Instruments and Methods in Physics Research*, 222:171–176, 1984.
  - [5] P. pukite J.M. Van Hove and P.I. Cohen. *RHEED streaks and instrument response*, pages 609–612. 1983.
  - [6] N. David Mermin Neil W. Ashcroft. *Solid State Physics*. Cengage Learning, 2011.
  - [7] T Almeida, Y Zhu, and P D Brown. Complementary RHEED and XRD investigation of  $\beta$ -FeOOH and  $\alpha$ -Fe<sub>2</sub>O<sub>3</sub> nanoparticles. *Journal of Physics: Conference Series*, 241:012087, jul 2010.
  - [8] Y. Kainuma. The theory of kikuchi patterns. *Acta Crystallographica*, 8:247–257, 1953.
  - [9] N. J. C. Ingle. Inelastic scattering techniques for *in situ* characterization of thin film growth: backscatter kikuchi diffraction. *Woodhead Publishing Seires in Electronic and Optical Materials*, pages 29–51, 2011.